Hydrol. Earth Syst. Sci. Discuss., 7, 6981–7006, 2010
www.hydrol-earth-syst-sci-discuss.net/7/6981/2010/
doi:10.5194/hessd-7-6981-2010

Hydrology and Earth System Sciences Discussions

Spatial variability in channel and slope morphology within the Ardennes Massif, and its link with tectonics

N. Sougnez and V. Vanacker

Université Catholique de Louvain, Earth and Life Institute, George Lemaître Centre for Earth and Climate Research, Louvain-la-Neuve, Belgium

Received: 27 August 2010 – Accepted: 2 September 2010 – Published: 16 September 2010

Correspondence to: N. Sougnez (nicolas.sougnez@uclouvain.be)

Published by Copernicus Publications on behalf of the European Geosciences Union.

Abstract

Geomorphic processes that produce and transport sediment, and incise river valleys are complex; and often difficult to quantify over longer timescales of 10^3 to 10^5 years. Morphometric indices that describe the topography of hill slopes, valleys and river channels have commonly been used to compare morphological characteristics between catchments and to relate them to hydrological and erosion processes. This work focuses on a wide range of slope and river channel morphometric indices to study their behavior and strength in regions affected by low to moderate tectonic activity. We selected 10 catchments of about 150 to 250 km^2 across the Ardennes Massif that cover various tectonic domains with uplift rates ranging from about 0.06 to 0.20 mm $year^{-1}$ since mid-Pleistocene times. The morphometric analysis indicates that the slope and channel morphology of third-order catchments is not yet in topographic steady-state, and exhibits clear convexities in slope and river profiles. Our data indicate that the fluvial system is the main driver of topographic evolution and that the spatial pattern of uplift rates is reflected in the distribution of channel steepness and convexity. The spatial variation that we observe in slope and channel morphology between the 10 third-order catchments suggests that the response of the fluvial system was strongly diachronous, and that a transient signal of adjustment is migrating from the Meuse valley towards the Ardennian headwaters.

1 Introduction

There is great interest across a broad spectrum of geoscience disciplines in unravelling the role of tectonic activity in driving erosion processes and landscape evolution (Burbank et al., 1996; Maddy, 1997; Vanacker et al., 2007a). Geomorphic processes that produce and transport sediment, and incise river valleys are complex; and often difficult to quantify over longer timescales of 10^3 to 10^5 years. Morphometric indices that describe the topography of hill slopes, valleys and river channels have commonly been used to compare morphological characteristics between catchments and to quantify their potential hydrologic behaviour (Horton, 1932, 1945; Douvinet et al., 2007). The development and spreading of numerical tools (particularly geographical information systems) has facilitated the widespread use of morphometric parameters in geoscience studies. Actually, a whole range of catchment and river parameters exists. Douvinet et al. (2005) have identified at least 57 reference indices that can be divided into 4 categories: shape (14), volumetric (19), network (9) and mixed indices (15).

More recently, those indices have been related to physical processes and landscape controls, such as stream-power models (Whipple and Tucker, 2002; Snyder et al., 2003; Whipple, 2004), stream sediment grain size variation (Surian, 2001; Rice and Church, 1998; Inoue, 1992; Petit et al., 2005), sea level and climate change (Bonnet and Crave, 2003; Roe et al., 2002; Whipple and al., 1999), and recent tectonic activity (Demoulin, 1998; Kirby and Whipple, 2001; Snyder et al., 2000). Most geomorphologic studies involving tectonic activity were concentrated in regions of high uplift rates and/or high denudation rates, such as the Himalayas (Burbank et al., 2003; Wobus et al., 2003; Lague and Davy, 2003), the Andes (Tibaldy and Leon, 2000; Kamp et al., 2005; Vanacker et al., 2007b), and the Alps (Schneider et al., 2008; Musumeci et al., 2002; Norton, 2008; Brocard and van der Beek, 2006). The link between tectonics, erosion and morphology has rarely been analyzed in regions of weak to moderate uplift rates (0.2–0.01 mm year^{-1}; Tebbens et al., 2000; Demoulin, 1998; Lague et al., 2000).

This work focuses on a wide range of slope and river channel morphometric indices to study their behavior and strength in regions affected by low to moderate tectonic activity. We analysed the spatial variation in slope and channel morphology for low relief terrain, and specifically tested if the present-day morphology can be used as an indicator of landscape response to tectonic activity. For these low relief landscapes with low uplift rates, we hypothesize that hill slope processes are the main drivers of topographic evolution and that the spatial pattern of uplift rates will be reflected in the distribution of slope steepness and local relief.

HESSD
7, 6981–7006, 2010

The Ardennes Massif is an excellent field site for studying geomorphic processes. The area has been subject to differential tectonic movement: the northeastern part of the Massif is characterized by moderate uplift rates and seismic activity, whereas the western and southern parts are undergoing only slight epeirogenic upheaval (Pissart, 1974; Demoulin, 1995; Meyer and Stets, 1998; Garcia-Castellanos et al., 2000). Various morphometric indices were derived to capture the spatial variation in slope and channel morphology within the Ardennes Massif. We analysed possible correlation between the rock uplift pattern and slope and river channel indices; and performed a cluster analysis to explore spatial aggregation of geomorphic response profiles in relation to the tectonic gradient observed by Demoulin and Hallot (2009).

2 Material and methods

2.1 Study area

The Ardennes Massif corresponds to the western part of the Rhenish shield which extends into Luxembourg and Germany (Fig. 1). The Cambrian massif consists of early Paleozoic metamorphic rocks, mostly phyllites and quartzites and is surrounded by Ordovician and early Devonian slates mainly to the south and east, and middle and late Devonian sandstones, shales and limestones in the north and west (Demoulin and Hallot, 2009). In this region, the North-Variscan fold-and-thrust belt has been superposed on structures from the old Caledonian orogeny. This results in a structurally complex basement where longitudinal ENE-WSW folds and thrust faults are cut by NW-SE to NNW-SSE striking normal faults (Demoulin, 1998).

The Variscan folding was followed by an erosional phase (Vandycke, 2002). From the Permian till the Early Cretaceous, the Ardennes remained almost constantly below sea level. After the retreat of the upper Cretaceous sea, stepped planation surfaces developed. Their present-day elevations indicate that the region underwent rock uplift of about 450 m, and locally even more than 500 m, since the Oligocene (Demoulin

HESSD
7, 6981–7006, 2010

and Hallot, 2009). Terrace sequences of rivers draining the Ardennes Massif suggest that uplift rates accelerated during the Quaternary, with an increase of uplift rates at the Pliocene-Pleistocene transition and at the beginning of the middle Pleistocene to reach maximum uplift of 0.5 mm $year^{-1}$ in the Northeast Ardennes (Demoulin et al., 2009). Geomorphic data derived from terrace sequences of incised fluvial systems were commonly used to infer the spatial pattern of Quaternary uplift (van Balen et al., 2000; Garcia-Castellanos et al., 2000). Demoulin and Hallot (2009) recently proposed a modification of the shape and amount of the Quaternary uplift of the Ardennes based on a new interpretation of the incision data of intra-massif streams and additional geomorphological data. Lithospheric folding in response to intraplate compression in front of the alpine orogen (Cloetingh et al., 2005; Demoulin and Hallot, 2009) and upwelling of the Eifel mantel plume (and thermal thinning of the lithospheric mantle, Meyer and Stets, 1998; Garcia-Castellanos et al., 2000) are commonly cited as the two main causes of the Quaternary uplift of the Ardennes Massif. Nowadays, the Ardennes-Rhenish Massif is characterized by a moderate seismic activity driven by intraplate motions (Camelbeeck, 2000; Cloetingh et al., 2005).

The presence of spatially relatively uniform (but temporally variable) climatic conditions during the Quaternary affords good opportunity to isolate the tectonic imprint on landscape evolution. We selected 10 catchments of about 150 to 250 km^2 across the Ardennes Massif (Fig. 1a: Aisne, Bocq, Hermeton, Hoegne, Hoyoux, Molignée, Salm, Vierre, Wamme and Warche rivers). Most catchments are third order catchments belonging to the Meuse River basin. Although the development of the Meuse river system started since the Eocene, the present day fluvial system was mainly established during the Pliocene period (Grimbérieux et al., 1995; Pissart, 1974, 1997). The selected catchments cover various tectonic domains with uplift rates ranging from about 0.06 to 0.20 mm $year^{-1}$ since mid-Pleistocene times according to the new map of post −0.73 Ma uplift by Demoulin and Hallot (2009).

HESSD
7, 6981–7006, 2010

2.2 Topographic and tectonic uplift data

Our morphometric study is based on the digital elevation model (DEM) provided by the Belgian National Geographical Institute (IGN). We used the DTM 1:10 000 product that is developed from photogrammetric derived levelling curves (IGN, 2008a). This product is a regular grid of data points at 20 m resolution, and is reported to have RMS errors between 0.5 and 1.25 m horizontally and 1 and 1.6 m vertically (IGN, 2008b). Because of interpolation artefacts in the original dataset, we reconstructed the initial levelling curves (at 5 m equidistance) from the digital elevation data. We interpolated the contour lines using the "Topo to Raster" ArcGis function to obtain a continuously varying 3-D surface. The DEM was then hydrologically corrected using the sink-fill method presented in Schaüble (2000). The drainage area of each catchment was derived from this DEM using the "Flow accumulation" ArcGIS function, while the transversal river and slope profiles were extracted using the "3-D Analyst" ArcGIS extension.

The spatial pattern of tectonic uplift (MU, in m, see Table 1) was derived from the uplift isolines presented by Demoulin and Hallot (2009). For each catchment, the average amount of uplift was calculated.

2.3 Morphometric parameters

First, simple morphometric indices that capture the overall slope morphology were derived. Classical morphometric indices (index of Gravelius, Schumm and Horton) were extracted to compare the overall 2-D geometrical shape between the catchments (Table 1). The indices of Schumm (Sc, in $m\,m^{-1}$) and Horton (Ho, in $m\,m^{-1}$) have the advantage of not being scale-dependent, which is not the case for the index of Gravelius (Gr, in $m\,m^{-1}$) that proved to be highly raster resolution dependent (Senadeera et al., 2004). To get an insight in the spatial distribution of the slope morphology within the catchments, slope and local relief maps were made (with local relief here defined as the relief in a 100 m range moving window). A local relief index (LRel, in m) was computed on the basis of the local relief map, and consists of the median value of all local relief values within the catchment.

Second, we focused on the river channel morphology. For each catchment we extracted the river longitudinal profiles and several transversal profiles based on the original levelling curves. The transversal topographic profiles were extracted perpendicularly to the river channel at sections that are not affected by local morphological changes related to river confluences. For each river, more than 20 transversal profiles were extracted. The eight most representative transversal profiles with minimal effect of anthropogenic artefacts (such as roads, reservoirs, or villages) were then selected for further analysis. Stream proximal slope (S_i, in %) and curvature (C_i, in m^{-1}) were calculated using the following equations:

$$S_i = \frac{(y_{i-1}) - (y_{i+1})}{(x_{i-1}) - (x_{i+1})} \cdot 100 \quad (1)$$

$$C_i = \frac{\left(\frac{(y_{i+2})-(y_i)}{(x_{i+2})-(x_i)}\right) - \left(\frac{(y_i)-(y_{i-2})}{(x_i)-(x_{i-2})}\right)}{(x_{i+2}) - (x_{i-2})} \quad (2)$$

with x_i = distance to source (m), and y_i = altitude (m) at point i.

Slope-Area diagrams were constructed to identify knick zones. Those knick zones are sections of the river channel that display an important increase in slope gradient, resulting from a difference in erosional power. Knickpoints can be created by different processes like lithological contrasts along the channel, heterogeneous sedimentary load, base level drops following sea level changes, and tectonic activity that can increase the relief locally or even regionally (Snyder et al., 2000; Whipple, 2004). The knickpoints with tectonic origin have been identified in the selected river channels using geologic maps and Slope-Area diagrams. For each river, we fitted an inverse power law equation (so-called Flint law) between the drainage area (A, in m) and the river

HESSD
7, 6981–7006, 2010

channel gradient (S, in m^2):

$$S = k_s A^{-\theta} \tag{3}$$

The empirically derived parameters k_s and θ are indicators of respectively the steepness and concavity of the river longitudinal profile (Flint, 1974; Hack, 1973; Whipple, 2004). Under steady-state conditions, a balance exists between local channel steepness and the upstream drainage area. The overall channel steepness k_s represents the relationship between net uplift and net erosion (Howard, 1994; Whipple and Tucker, 1999). A comparison of the observed Slope-Area relationships for the 10 rivers in the Ardennes Massif allows us to compare the channel morphology of rivers draining highly different tectonic regimes. As the empirically derived value of the steepness index (k_s) has been proved to be dependent on the profile concavity, we normalised the steepness values (k_{sn}) to a reference concavity, θ_r, of 0.45 following Snyder et al. (2000) and Kirby et al. (2000). The normalised steepness values, k_{sn}, can then be used to compare the steepness between different river systems; with larger values of k_{sn} representing steeper rivers.

In addition to these parameters, we derived an area-normalized stream concavity index (SCI) of each river channel as defined by Demoulin (1998) and Zaprowski et al. (2005). The form of the river channels in the Ardennes Massif is highly variable, and some rivers display clear convexities (also called knick zones). Figure 1b illustrates the longitudinal profile of all the studied rivers including the location of the main knickpoint. The SCI is a measure of the surface between the normalised longitudinal profile and a straight line joining the source and the outlet of the catchment (Eq. 4):

$$SCI_i = 1 - \sum_{i=0}^{1} ((x_i - x_{i+1})(y_i + y_{i+1})) \tag{4}$$

with x_i = distance to source (m), and y_i = altitude (m) at point i. If the stream profile is above the reference line, the area between the two is considered negative. A river profile with positive SCI value will be considered as concave up, and a negative value

HESSD
7, 6981–7006, 2010

is an indicator of a convex up river profile (Zaprowski et al., 2005). We slightly modified the initial formulation of the index so that the values are comprised between ±1, with an equilibrium concave up longitudinal profile having a SCI of about 0.5. Obviously, the behaviour of the index remains similar.

Third, we analysed the hypsometry of the catchments to get a measure of the overall slope and channel morphology. The hypsometric integral, HI, was calculated as follows:

$$\mathrm{HI}_i = \sum_{i=0}^{1} \frac{1}{2}(y_{i+1} + y_i)(x_{i+1} - x_i) \quad (5)$$

where x_i = distance to source (m), and y_i = altitude (m). The hypsometric integral is a measure of the distribution of landmass volume above a basal reference plane, and can be interpreted in terms of relative landform age (Strahler, 1952). Differences in the shape of the hypsometric curve have been related to differences in erosive and tectonic processes (Weissel et al., 1994), and the value of the hypsometric integral has been interpreted as an indicator of the degree of disequilibrium in the balance between erosive and tectonic forces for a particular landform (Luo, 1998). When comparing the morphology of catchments, the catchment with the largest value of HI has the largest amount of landmass above the outlet, and this can be interpreted in terms of lower erosion or higher tectonic activity. As our catchments have comparable size (150 to 250 km^2), the scale-dependency of the hypsometric integral should not directly affect our results.

In addition to the morphometric indices that are described above, we calculated two parameters that are linked to the position of the knick zone: Ach and Rch, respectively the absolute (i.e. height above sea level, m) and relative (i.e. height above the altitude of the catchment outlet, m) height of the main stream convexity.

HESSD
7, 6981–7006, 2010

N. Sougnez and V. Vanacker

2.4 Statistical analyses

In order to test the possible link between the tectonic activity and the catchment morphology, we applied correlation and spatial clustering techniques. We performed a correlation analysis to evaluate the correlation between the morphometric parameters and the MU of the catchments. A multivariate clustering technique was applied to identify the indices that are most likely to represent the observed spatial variability in slope and channel morphology. We used the Ward's classification procedure to identify the optimal number of profile types, and a K-means clustering method to recognize the weight of each parameter in the classification process (Lu et al., 2004).

3 Results

Our morphometric analysis indicates that large differences exist in slope and channel morphology both within and between the selected catchments (Fig. 1, Table 1). The catchments in the western and southern part of the Ardennes Massif are more prone to have relatively smooth river and channel profiles, although various exceptions exist. In the northeastern part of the Ardennes Massif, we observed various catchments with irregular "non-equilibrium" slope and channel profiles, and the presence of clear knick zones.

We observe that the absolute height of the river channel convexity is related to the mean uplift: catchments that are located in regions with higher uplift rates generally have knick zones at higher altitude (Fig. 2a). This relationship may seem self-evident, as the mean elevation of the catchment is expected to be directly related to the total amount of uplift. However, this observation also implies that knickpoints do not dissipate rapidly in low relief terrain with low to moderate uplift rates.

We observed also some correlation between the mean uplift of the catchments and the stream concavity index: catchments with concave up river profiles are generally located in zones with low uplift rates (Fig. 2b). However, convex reaches are not

HESSD
7, 6981–7006, 2010

necessarily associated with zones of high uplift rates (two circles in Fig. 2b). This might partially be explained by the presence of local lithological contrasts, but might also be associated with local tectonic activity (Bocq and Hoyoux catchments, located close to subsidence centre in Namur area). The latter is still under study (Pissart and Lambot, 1989; Demoulin, 1998), and is not represented in the data of Demoulin and Hallot (2009).

A K-means cluster analysis was performed to identify groups of catchments with similar patterns of slope and channel morphology. A reduced number of variables was selected to avoid auto-correlation in the analysis: Rch, Ho, k_{sn}, HI and SCI. Those parameters are representative of the various aspects of the slope and channel morphology: Rch for the river knickpoint position, Ho as a measure of the shape of the catchment, k_{sn} as an index for the general slope (steepness) of the river channel, HI as a measure of the catchment relief and SCI as an index of the general form of the river longitudinal profile. Table 2 shows the main characteristics of the three clusters that were recognized by the statistical procedure, and gives the mean value and the standard deviation associated to each cluster.

When analysing the three statistical clusters in a slope-area diagram (Fig. 2d), we observe that they each cover a different domain. The second cluster (Bocq, Warche, Hoyoux and Salm, represented with black dots Fig. 2d) is characterized by a low concavity index ($\theta = 0.34$) opposed to concavities of 0.45 and 0.43 of the 1st (Aisne, Wamme and Hoegne, grey dots) and 3rd cluster (Hermeton, Molignée and Vierre, black crosses) respectively. Cluster 2 also differs from the other clusters in its steepness value (k_{sn}). Actually, a river with low intercept (i.e. $k_{sn} = 4$) can be interpreted as having a greater steepness of its longitudinal profile. The statistical clusters correspond to different tectonic domains in the Ardennes Massif (Fig. 1a). The first and second cluster contain mainly rivers that are draining the most uplifted part of the Ardennes Massif, while the third cluster contains exclusively Condruzian rivers and the Vierre, which is located further upstream in the Semois river system (Fig. 3).

HESSD
7, 6981–7006, 2010

4 Discussion

Our data on the river and channel morphology from a region with differential uplift rates indicate that the interaction between tectonic activity, slope and river processes is complex. The variability that we observe in slope morphology within the Ardennes Massif is not able to fully capture the complex response of the landscape to the tectonic imprint. The combination of different morphometric indices in a multivariate cluster analysis reveals interesting results. The region of highest uplift rates is located in the northeastern part, and is characterized by high values of local relief (Fig. 2c) and steep river channels displaying clear convexities in the upper part of their river long profiles.

Despite the long-term uplift of the Ardennes Massif at low to moderate rates, the slope and channel morphology of third-order catchments is not yet in topographic steady-state, and exhibits clear convexities (or knickzones) in slope and river profiles (Fig. 1). Hence, the spatial variation that we observe in slope and channel morphology between the 10 third-order catchments is potentially not only the direct result of the differential uplift pattern, but might also reflect the transient response of the catchments to relative base level lowering.

The Meuse River that is draining the third-order catchments acts as the local base level to which the fluvial system is adapting after the post 0.73 Ma tectonic uplift of the western Rhenish shield and the Ardennes (Fig. 1). Figure 3 clearly shows that the knick zones in the tributaries of the Meuse River are located at different heights, with the highest knick zones located in the northeastern part of the Ardennes Massif. This suggests that the response of the fluvial system was strongly diachronous, and that a transient signal of adjustment is migrating from the Meuse valley towards the Ardennian headwaters. This hypothesis is consistent with recent insights from ^{10}Be/^{26}Al dating of the Younger Main Terrace (YMT, frequently used geomorphic marker see Rixhon et al., 2009) of several Ardennian rivers. The absolute ages that Rixhon et al. (2010) obtain for the same terrace level within the Ardennes are significantly younger in the hydrologically more distant parts of the lower Meuse valley, which suggests that the quaternary incision in the uplifted Ardennes Massif occurs diachronous.

HESSD
7, 6981–7006, 2010

Finally, our data show some correlation between the overall river morphology and knickpoint migration. We broadly identified three types of catchments based on hypsometric and river channel analysis, and observed a nonlinear relation between the hypsometric integral, HI, and the relative position of the stream convexity, Rch (Fig. 4). The first morphological type (low HI, and low position of the convexity) broadly corresponds to river catchments with equilibrium long profiles. Three catchments (Vierre, Hermeton, and Molignée) in the upper part of the Meuse catchment have such channel morphology, and seem not yet affected by the base level changes following the uplift of the Ardennes Massif. The second type (high HI, medium relative height of convexity) contains catchments that were subject to recent tectonic activity (Bocq and Hoyoux) or that had higher tectonic uplift rates (Warche and Salm). The rivers that are draining regions with weaker lithologies or long incision history appear in the third group. This theoretical model also indicates that the hypsometric integral alone is not adequate to determine the relative landform age or the adaptation stage of a river profile. Low values of the hypsometric integral may be present in catchments that are influenced by a tectonically-driven knickpoint (1st cluster), or that have not yet been affected by the uplift and thus remained in equilibrium state (3rd cluster). This also highlights that a multivariate analysis, including HI, is necessary to fully understand the link between slope and channel morphology and tectonic activity.

When we synthesize our observations of the slope and channel morphology of the selected catchments, we can broadly identify three morphological groups (indicated as A, B, C; in Fig. 5). The slope and channel morphology of these groups can be interpreted in terms of transient adjustment of the topography to relative base level change following uplift (Fig. 5). The first slope and channel morphology group (A) is typical for catchments that are located in the upper part of the catchments where a smooth channel-to-hillslope transition could be observed. This morphology was mostly observed for plateau positions, and corresponds to alluvial stream systems where slope and channel processes are coupled. The second and third group are transitional systems. The B scheme is characterized by very high and constant slopes close to the

HESSD
7, 6981–7006, 2010

rivers and by a rapid transition to flat slopes. This scheme is typical for knick zones with a decoupling of channel and slope processes. The C scheme (smooth S-curved slopes) can be seen as the later stage of evolution of the B scheme with the development of a large valley plain and with the highest slope gradients located at the middle part of the slopes. We found this C scheme often in the downstream part of the catchments, and it corresponds to recent rejuvenated topography. A similar study by Norton et al. (2008) characterized the basin morphometrics of a transient landscape in the forelands of the Swiss Alps, and indicated that the local hillslope curvature and slope angles can be used as a proxy for the degree of rejuvenation in a catchment. Our study confirms the strength of stream proximal curvatures and stream proximal slopes as morphometric indices of relief rejuvenation, but indicates that several forms of hillslope channel coupling can coexist within the same catchment based on the transient state of adjustment to relative base level change.

5 Conclusions

Our morphometric analysis of 10 catchments in the Ardennes Massif indicates that slope and channel morphology is an indicator of transient adjustment of rivers to tectonic uplift. Whereas there is some general agreement between some of the overall morphometric parameters and the mean uplift rates for the Ardennes Massif, the detailed picture is far more complex and some metrics appear to be insensitive to differential tectonic uplift. Our data show that river channel properties (river longitudinal and transversal profiles) are better indicators of recent tectonic activity than the general hillslope form and relief. Moreover, longitudinal profiles and knickpoint retreat analysis have shown that the fluvial system plays an important role in the shape pattern of the studied catchments. Rivers that are located far in the hydrological network seems to be in equilibrium state, or in the first stages of a transient adjustment with a knickzone located in the lowest part of the catchments.

HESSD

7, 6981–7006, 2010

Acknowledgements. This study is part of a PhD research project that deals with the link between topography, tectonics and erosion in the Ardennes Massif. This project is financed by a Fonds spécial de recherche grant of the Université de Louvain to VV.

References

Bonnet, S. and Crave, A.: Landscape response to climate change: Insights from experimental modeling and implications for tectonic versus climatic uplift of topography, Geology, 31, 123–126, 2003.

Brocard, G. and van der Beek, P.: Influence of incision rate, rock strength and bedload supply on bedrock river gradients and valley-flat widths: Field-based evidence and calibrations from western Alpine rivers (SE France), Tectonics, in: Climate and Landscape Evolution, edited by: Willett, S. D., Hovius, N., Brandon, M. T., and Fisher, D., eds., Geol. Soc. Am. Spec. Publ., 398, 101–126, 2006.

Burbank, D., Leland, J., Fielding, E., Anderson, R., Brozovic, N., Reid, M., and Duncan, C.: Bedrock incision, rock uplift and threshold hillslopes in the northwestern Himalayas, Nature, 379, 505–510, 1996.

Burbank, D., Blythe, A., Putkonen, J., Pratt-Sitaula, B., Gabet, E., Oskin, M., Barros, A., and Ojha, T.: Decoupling of erosion and precipitation in the Himalayas, Nature, 426, 652–655, 2003.

Camelbeeck, T., Alexander, P., Vanneste, K., and Meghraoui, M.: Long term seismicity in regions of present day low seismic activity: the example of western Europe, Soil Dyn. Earthqu. Eng., 20, 405–414, 2000.

Cloetingh, S., Ziegler, P., Beekman, F., Andriessen, P., Hardebol, N., and Dèzes, P.: Intraplate deformation and 3D rheological structure of the Rhine Rift System and adjacent areas of the northern Alpine foreland, Int. J. Earth Sci., 94, 758–778, 2005.

Demoulin, A.: L'Ardenne des Plataux, heritage des temps anciens, surfaces d'érosion en Ardennes, edited by: Demoulin, A., in: L'Ardenne, essai de géographie physique, Dep. Géogr. Phys. Quat., Univ. Liège, 1995.

Demoulin, A.: Testing the tectonic significance of some parameters of longitudinal river profiles: the case of the Ardenne (Belgium, NW Europe), Geomorphology, 24, 189–208, 1998.

Demoulin, A. and Hallot, E.: Slope and amount of the Quaternary uplift of the western Rhenish shield and the Ardennes (western Europe), Tectonophysics, 474, 696–708, 2009.

Demoulin, A., Hallot, E., and Rixhon, G: Amount and controls of the Quaternary denudation in the Ardennes massif (western Europe), Earth Surf. Proc. Land, 34, 1487–1496, 2009.
Douvinet, J., Delahaye, D., and Langlois, P.: Catchment morphgology and dynamics of hyper-concentrated stream flows on loamy plateaux (Basin Paris, in the North-Westren part of France), Sixth International Conference on Geomorphology (ICG), “Geomorphology in regions of environmental contrasts”, 7–11 September, Zaragoza, Espagne, 2005.
Douvinet, J., Delahaye, D., and Langlois, P.: De la morphométrie à un champ de mesure de la structuration d'un bassin versant, Actes du Colloque International de Géomatique et d'Analyse Spatiale (SAGEO'2007), 18–20 June, Clermont-Ferrand, 2007.
Flint, J.: Stream gradient as a function of order, magnitude, and discharge, Water Resour. Res., 10, 969–973, 1974.
Garcia-Castellanos, D., Cloetingh, S., and van Balen, R.: Modelling the Middle Pleistocene uplift in the Ardennes-Rhenish Massif: thermo-mechanical weakening under the Eifel?, Global Planet. Change, 27, 39–52, 2000.
Grimbérieux, J., Laurant, A., and Ozer, P.: Les rivières s'installent. In : L'Ardenne. Essai de géographie physique. Hommage au professeur Pissart, A. (Demoulin, A., édit.), Département de géographie physique et du Quaternaire, Université de Liège, 238 pp., 1995.
Hack, J.: Stream-profile analysis and stream-gradient index, US Geol. Sur. J. Res., 1, 421–429, 1973.
Horton, H.: Drainage basin characteristics, Trans. Amer. Geophys Union, 13, 350–361, 1932.
Horton, H.: Erosional development of streams and their drainage basins, Geol. Soc. Am. Bull., 56, 275–370, 1945.
Howard, A., Dietrich, W., and Seidl, M.: Modeling fluvial erosion on regional to continental scales, J. Geophys. Res., 99, 13971–13986, 1994.
IGN: Website of the National Geographical Institute of Belgium: last visit on 13 April 2008: www.ngi.be, 2008a.
IGN: DTM 1:10.000 Wallonie, Technical report provided by the National Geographical Institute of Belgium, last update 14 may 2008, 2008b.
Inoue, K.: Downstream change in grain size of river bed sediments and its geomorphological implications in the Kanto Plain, central Japan, Geographical Review of Japan, 65, 75–89, 1992.
Kamp, U., Bolch, T., and Olsenholler, J.: Geomorphometry of Cerro Sillajhuay, Chile/Bolivia: comparison of DEMs derived from ASTER remote sensing data and contour maps, Geocarto

International, 20, 23–34, 2005.
Kirby, E. and Whipple, K.: Quantifying differential rock-uplift rates via stream profile analysis, Geology, 29, 415–418, 2001.
Kirby, E., Whipple, K., Burchfiel, B., Tang, W., Berger, G., Sun, Z., and Chen, Z.: Neotectonics of the Min Shan, China: Implications for mechanisms driving Quaternary deformation along the eastern margin of the Tibetan Plateau, Geol. Soc. Am. Bull., 112, 375–393, 2000.
Lague, D. and Davy, P.: Constraints on the long-term colluvial erosion law by analyzing slope-area relationships at various tectonic uplift rates in the Siwaliks Hills (Nepal), J. Geophys. Res., 108, 2129, doi:10.1029/2002JB001893, 2003.
Lague, D., Davy, P., and Crave, A.: Relationships between average topographic forms and lithological and tectonic controls. Examples from Brittany (France) and numerical modelling, Phys. Chem. Earth, 25, 543–548, 2000.
Luo, W.: Hypsometric analysis with a Geographic Information System, Comput. Geosci., 24, 815–821, 1998.
Lu, Y., Lu, S., Fotouhi, F., Deng, Y., and Brown, S.: FGKA: A Fast Genetic K-means Algorithm, in Proc. of the 19th ACM Symposium on Applied Computing, 162–163, Nicosia, Cyprus, 2004.
Maddy, D.: Uplift-driven valley incision and river terrace formation in southern England, J Quaternary Sci., 12, 539–545, 1997.
Meyer, W. and Stets, J.: Junge Tektonik im Rheinischen Schiefergebirge und ihre Quantifizierung, Zeitschrift der Deutschen Geologischen Gesellschaft, 149, 359–379, 1998.
Musumeci, G. and Colombo, F.: Late Visean mylonitic granitoids in the Argentera Massif (Western Alps): age and kinematic constraints on the Fèrriere Mollière shear zone, Cr. Acad. Sci. II A, 334, 213–220, 2002.
Norton, K., von Blanckenburg, F., Schlunegger, F., Schwab, M., and Kubik, P.: Cosmogenic nuclide-based investigation of spatial erosion and hillslope channel coupling in the transient foreland of the Swiss Alps, Geomorphology, 95, 474–486, 2008.
Petit, F., Gob, F., Houbrechts, G., and Assani, A.: Critical specific stream power in gravel-bed rivers, Geomorphology, 69, 92–101, 2005.
Pissart, A.: La Meuse en France et en Belgique. Formation du basin hydrographique. Les terraces et leurs enseignements, in: Centenaire de la Soc. Géol. De Belg. L'évolution quaternaire des basins fluviaux de la mer du Nord méridionale, edited by: Macar, P., Liège, Belgium, 105–131, 1974.

HESSD
7, 6981–7006, 2010

Spatial variability in channel and slope morphology

N. Sougnez and V. Vanacker

Pissart, A. and Lambot, P.: Les mouvements actuels du sol en Belgique; comparaison de deux nivellements IGN (1946–1948 et 1976–1980), Ann. Soc. Géol. Belg., 112, 495–504, 1989.
Pissart, A., Harmand, D., and Krook, L.: L'évolution de la Meuse de Toul à Maastricht depuis le Miocène. Corrélations chronologiques et traces des captures de la Meuse lorraine d'après les minéraux denses, Géographie Physique et Quaternaire, 51, 267–284, 1997.
Rice, S. and Church, M., Grain size along two gravel-bed rivers: statistical variation, spatial pattern and sedimentary links, Earth Surf. Proc. Land., 23, 345–363, 1998.
Rixhon, G., Braucher, R., Siame, L., Bourlès, D., and Demoulin, A.: 10Be and 26Al dating of river terraces and quaternary incision rates in the Ardenne massif (eastern Belgium), Geophysical Research Abstracts, EGU General Assembly 2009, Vol.11–EGU2009-9419, 2009.
Rixhon, G., Bourlès, D., Braucher, R., Siame, L., Bovy, B., and Demoulin, A.: Quaternary river incision in the uplifted Rhenish massif (Ardennes, Belgium) – Insights from 10Be/26Al dating of river terraces, Geophysical Research Abstracts, EGU General Assembly 2010, Vol.12–EGU2010–11419, 2010.
Roe, G., Montgomery, D., and Hallet, B.: Effects of orographic precipitation variations on the concavity of steady-state river profiles, Geology, 30, 143–146, 2002.
Senadeera, K., Piyasiri, S., and Nandalal, K.: The evaluation of Morphmetric Characteristics of Kotmale Reservoir catchment using GIS as a tool, Sri Lanka, The International Archives of the Photogrammetry, Remote Sensing and Spatial Information Sciences, 34, 2004.
Schäuble, H.: Erosionsmodellierungen mit GIS, Probleme und Lösungen zur exakten Prognose von Erosion und Akkumulation, in: Ergebnisse der Jahrestagung des Arbeitskreises GIS 25/26, Tübingen, 51–62, 2000.
Schneider, H., Schwab, M., and Schlunegger, F.: Channelized and hillslope sediment transport and the geomorphology of mountain belts, Int. J. Earth. Sci., 97, 179–192, 2008.
Snyder, N., Whipple, K., Tucker, G., and Merritts, D.: Landscape response to tectonic forcing: DEM analysis of stream profiles in the Mendocino Triple junction region, Northern California, Geol. Soc. Am. Bull., 112, 1250–1263, 2000.
Snyder, N., Whipple, K., Tucker, G., and Merritts, D.: Channel response to tectonic forcing: field analysis of stream morphology and hydrology in the Mendocino triple junction region, northern California, Geomorphology, 53, 97–127, 2003.
Strahler, A.: Hypsometric (area-altitude) analysis of erosional topology, Geol. Soc. Am. Bull., 63, 1117–1142, 1952.
Surian, N.: Downstream variation in grain size along an Alpine river: analysis of controls and

HESSD
7, 6981–7006, 2010

Spatial variability in channel and slope morphology

N. Sougnez and V. Vanacker

processes, Geomorphology, 43, 137–149, 2001.
Tebbens, L., Veldkamp, A., Van Dijke, J., and Schoorl, J.: Modeling longitudinal-profile development in response to Late Quaternary tectonics, climate and sea-level changes: the River Meuse, Global Planet. Change, 27, 165–186, 2000.
Tibaldi, A. and Leon, J.: Morphometry of late Pleistocene – Holocene faulting and volcanotectonic relationship in the southern Andes of Colombia, Tectonics, 19, 358–377, 2000.
Van Balen, R., Houtgast, R., Van der Wateren, F., Vandenberghe, J., and Bogaart, P.: Sediment budget and tectonic evolution of the Meuse catchment in the Ardennes and the Roer Valley Rift System, Global Planet. Change, 27, 113–129, 2000.
Vanacker, V., von Blanckenburg, F., Hewawasam, T., and Kubik, P.: Geomorphic development of the Sri Lanka Central Highlands, Earth Planet. Sc. Lett., 253, 402–414, 2007a.
Vanacker, V., von Blanckenburg, F., Govers, G., and Kubik, P.: Transient landscape evolution following uplift in the Southern Ecuadorian Andes, Geochim. Cosmochim. Ac., 71, A1052, doi:10.1016/j.gca.2007.06.028, 2007b.
Vandycke, S.: Palaeostress records in Cretaceous formations in NW Europe: extensional and strike-slip events in relationships with Cretaceous-Tertiary inversion tectonics, Tectonophysics, 357, 119–136, 2002.
Weissel, J., Pratson, L., and Malinverno, A.: The length-scaling properties of topography, J. Geophys. Res., 99, 13997–14012, 1994.
Whipple, K.: Bedrock rivers and the geomorphology of active orogens, Annual review of earth and planetary sciences, 32, 151–185, 2004.
Whipple, K., Kirby, E., and Brocklehurst, S.: Geomorphic limits to climate-induced increases in topographic relief, Nature, 401, 39–43, 1999.
Whipple, K. and Tucker, G.: Dynamics of the Stream Power River Incision Model: Implications for Height Limits of Mountain Ranges, Landscape Response Timescales and Research Needs, J. Geophys. Res., 104, 17661–17674, 1999.
Whipple, K. and Tucker, G.: Implications of sediment-flux-dependent river incision models for landscape evolution, J. Geophys. Res., 107, B2, doi:10.1029/2000JB000044, 2002.
Wobus, C., Hodges, K., and Whipple, K.: Has focused denudation sustained active thrusting at the Himalayan topographic front, Geology, 31, 861–864, 2003.
Zaprowski, B., Pazzaglia, F., and Evenson, E.: Climatic influences on profile concavity and river incision, J. Geophys. Res., 110, F03004, doi:10.1029/2004JF000138, 2005.

HESSD
7, 6981–7006, 2010

Spatial variability in channel and slope morphology

N. Sougnez and V. Vanacker

Table 1. Morphometric indices: S = surface; P = perimeter; MU = mean uplift (according to Demoulin and Hallot, 2009); Ach and Rch = the absolute and relative height of the convexities (in meters); LRel = the median of the local relief in a 100 m range window; ho = the altitude of outlet; Gr, Ho and Sc = the classical morphometric indices (Gravelius, Horton and Shumm); θ and Ksn = convexity and normalised steepness indices (Flint law); HI = the hypsometry integral; and SCI = the stream convexity index.

Rivers	S (km^2)	P (km)	MU (m)	Ach (m a.s.l.)	Rch (m)	LRel (m)	ho (m a.s.l.)	Gr ($m\,m^{-1}$)	Ho ($m\,m^{-1}$)	Sc ($m\,m^{-1}$)	θ (–)	Ksn (–)	HI (–)	SCI (–)
Aisne	190.6	71.0	114.77	450	315	10.85	135	1.439	0.441	0.750	0.478	44.45	0.251	0.379
Bocq	235.4	89.0	84.41	195	100	6.62	95	1.624	0.341	0.659	0.478	11.87	0.523	−0.055
Hermeton	169.3	69.6	69.19	150	50	4.72	100	1.498	0.316	0.635	0.323	13.25	0.442	0.165
Hoegne	208.6	75.1	109.54	510	375	7.83	135	1.456	0.356	0.673	0.552	72.19	0.221	0.316
Hoyoux	255.7	94.6	86.38	200	125	5.20	75	1.656	0.570	0.852	0.017	26.15	0.481	0.002
Molignée	139.3	58.5	70.25	150	60	6.01	90	1.388	0.384	0.699	0.138	18.77	0.376	0.145
Salm	238.0	90.3	133.49	460	210	7.12	250	1.640	0.423	0.734	0.052	24.39	0.422	−0.002
Vierre	259.1	89.2	102.58	330	10	6.27	320	1.551	0.374	0.690	0.519	13.62	0.263	0.408
Wamme	140.2	68.8	109.31	430	245	7.83	185	1.627	0.440	0.748	0.196	38.93	0.308	0.178
Warche	191.2	94.7	145.84	522.5	222.5	6.30	300	1.918	0.245	0.558	0.513	11.12	0.484	0.011

HESSD
7, 6981–7006, 2010

N. Sougnez and V. Vanacker

Table 2. Clusters characteristics (values of mean and standard deviation of the parameters).

Cluster	Rivers		Rch	Ho	Ksn	HI	SCI
1	Aisne, Wamme, Hoegne	Mean	311.7	0.412	51.9	0.260	0.291
		StD	65.06	0.049	17.8	0.044	0.103
2	Bocq, Warche, Hoyoux, Salm	Mean	164.4	0.395	18.4	0.478	−0.011
		StD	60.98	0.138	8.0	0.042	0.030
3	Hermeton, Molignée, Vierre	Mean	40.00	0.358	15.2	0.360	0.239
		StD	26.46	0.037	3.1	0.091	0.146

HESSD
7, 6981–7006, 2010

Spatial variability in channel and slope morphology

N. Sougnez and V. Vanacker

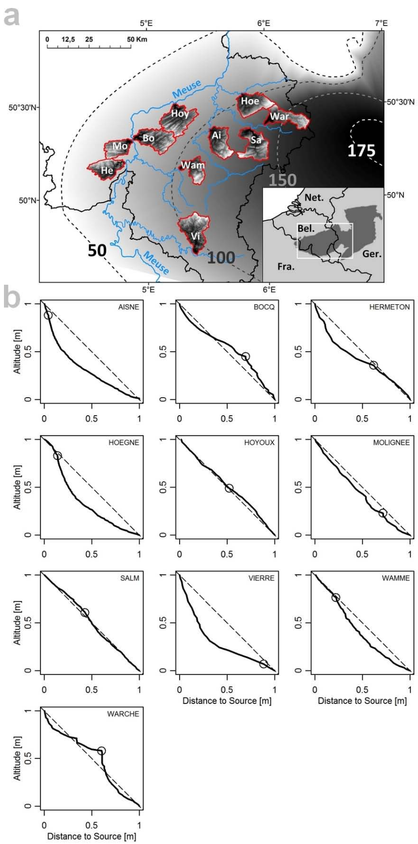

Fig. 1. (a) Location of the 10 catchments in the Ardennes-Rhenish Massif (inset map). The dotted lines correspond to the uplift isolines (values in meters) from Demoulin and Hallot (2009), and were derived from terrace sequences. **(b)** Normalised longitudinal profiles of the 10 selected rivers with location of the main channel convexity (circle).

HESSD
7, 6981–7006, 2010

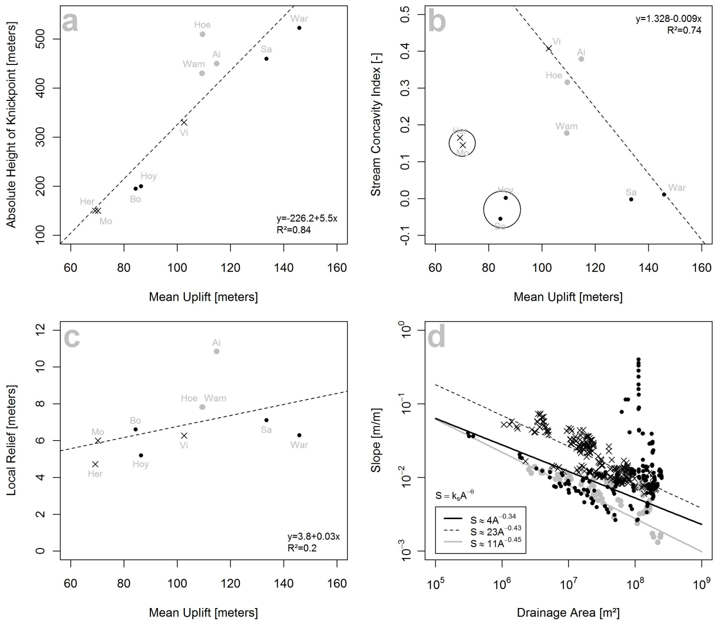

Fig. 2. (a) Relation between the absolute height of the knickpoint and the mean uplift (MU). **(b)** Relation between the stream concavity index and (SCI) and the mean uplift (MU). The dotted line represents the expected relationship between the two indices **(c)** Relation between the local relief (*LRel*) and the mean uplift (MU). **(d)** Illustration of the three cluster groups within the Slope-Area space. The grey dots represent the first cluster (Aisne, Wamme and Hoegne rivers), the black dots the second cluster (Bocq, Warche, Hoyoux and Salm rivers), and the black crosses represent the third cluster (Hermeton, Molignée and Vierre rivers).

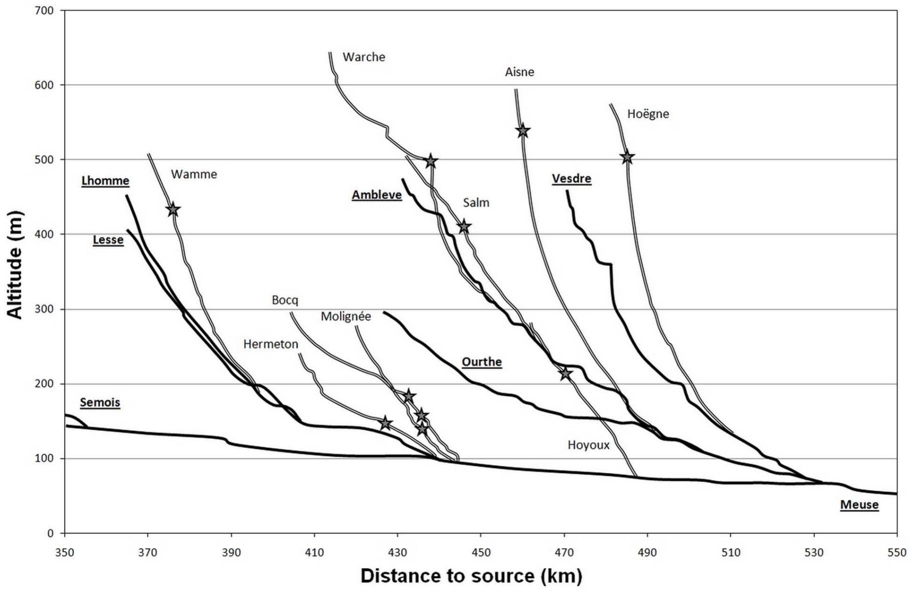

Fig. 3. Longitudinal profiles of the selected rivers within the Meuse river catchment. Double lines represent the selected rivers, bold lines the major streams of the region and stars indicate the position of the main knickpoint within each river profile. The Vierre profile is not represented in this graphic because of its distant location in the Semois river system.

HESSD
7, 6981–7006, 2010

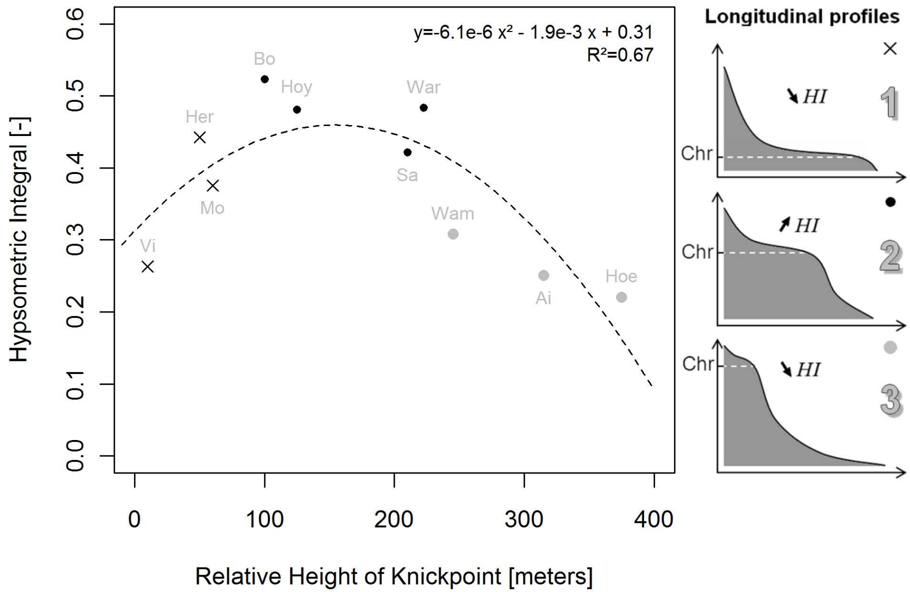

Fig. 4. Nonlinear relation between the relative height of the channel convexity (Rch) and the hypsometric integral (HI). Three phases of knickpoint upward migration are represented in the right panel.

HESSD
7, 6981–7006, 2010

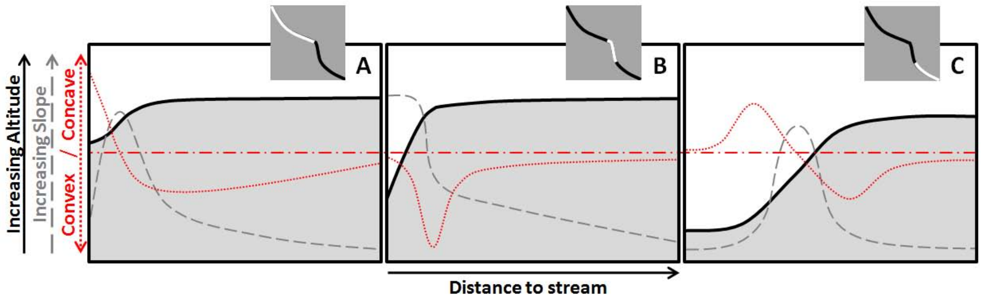

Fig. 5. Schematic representation of the change in hill slope morphology measured perpendicular to the river channel for three different positions: **(A)** above the river channel knick zone, **(B)** in the knick zone and **(C)** below the knick zone. The valley cross profiles are shown by the black line, the changes in stream proximal slopes by the dashed grey line and the stream proximal curvature by the red dotted line.

HESSD
7, 6981–7006, 2010